Condensed Matter Physics 2007, Vol. 10, No 1(49), pp. 11–16

CONDENSED MATTER PHYSICS

Phonon spectra of Cu_6PS_5Br superionic ferroelastic: experimental and theoretical studies

I.P.Studenyak*[1], K.Z.Rushchanskii[2], R.Yu.Buchuk[1], V.O.Stephanovich[2]

[1] Uzhgorod National University, Faculty of physics, 46 Pidhirna Str., 88000 Uzhgorod, Ukraine

[2] Institute for Solid State Physics and Chemistry, Uzhgorod National University, 54 Voloshyn Str., 88000 Uzhgorod, Ukraine

Received September 4, 2006

The anomalous temperature behavior of the Raman scattering bands at superionic phase transition of Cu_6PS_5Br is revealed. Using density functional perturbation theory within local density approximation, *ab initio* long-wavelength phonons have been obtained for high-symmetry cubic structure. In the calculated phonon spectrum two unstable modes indicate the experimentally observed sequence of ferroelastic and superionic phase transitions.

Key words: *superionic materials, lattice dynamics, phase transitions*

PACS: *63.20.Dj, 64.60.Cn, 78.30.Hv*

1. Introduction

Cu_6PS_5Br crystals belong to the family of compounds with argyrodite structure [1,2]. They are characterized by high concentration of disordered vacancies and possess both superionic and ferroelastic properties. High ionic conductivity at room temperature [3,4] determines the possibility of their application as solid electrolyte sources of energy, sensors and capacitors. At room temperature these crystals belong to cubic syngony (space group $F\overline{4}3m$) while at low temperatures two phase transitions (PTs) are realized: a ferroelastic transition at $T_c = (268 \pm 2)$ K and a superionic one at $T_s = (166 - 180)$ K [3,4]. Below the ferroelastic PT temperature Cu_6PS_5Br crystals belong to monoclinic syngony (space group Cc), and the superionic PT reveals the features of an isostructural transformation [5]. The ferroelastic PT is a second order transition, as indicated by a typical temperature behavior of specific heat, dielectric constant and elastic properties [3–10]. At $T = T_c$ domains appear in the crystal structure. The results of electrical, dielectric, calorimetric, acoustic and optical properties of Cu_6PS_5Br crystals were presented in references [3–10]. The present paper is aimed at the experimental and theoretiacal studies of phonon spectra in Cu_6PS_5Br superionic ferroelastics.

2. Experimental and computational details

Cu_6PS_5Br single crystals were grown using chemical vapor transport method. Raman scattering measurements were performed on a LOMO DFS-24 grating monochromator, the excitation being provided by a He-Ne laser (632.8 nm) [4]. The spectral slit did not exceed 1 cm^{-1}. An UTREX cryosystem was applied for the low-temperature studies.

The ground state and vibrational properties were investigated in the plane-wave approximation of the density functional theory [11]. The non-local *ab initio* norm-conserving pseudopotentials in the Troulier-Martins form were used [12]. The $4s^2 3d^{10}$, $3s^2 3p^3$, $3s^2 3p^4$ and $4s^2 4p^5$ electron configurations were used for valence electrons for the Cu, P, S and Br atoms, respectively. The

*E-mail: studenyak@dr.com

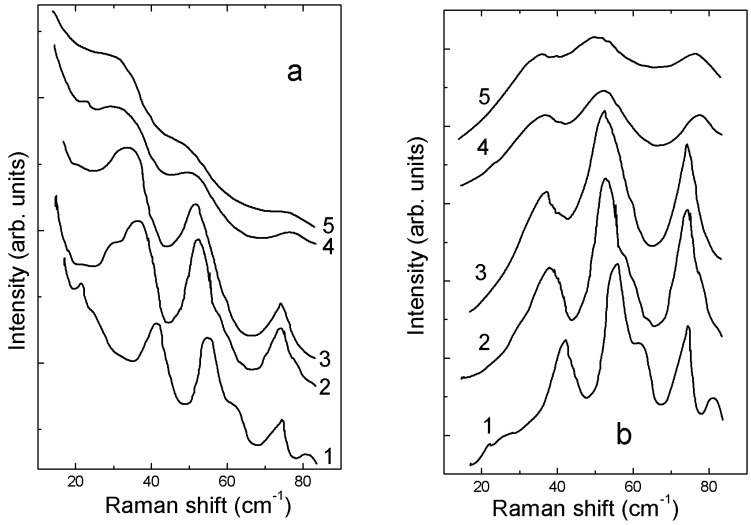

Figure 1. Raman spectra of Cu_6PS_5Br crystal, directly measured experimentally (a) and corrected for Bose-Einstein statistic factor (b) in the low-frequency range ($\omega < 100$ cm^{-1}) at the temperatures 77 K (1), 140 K (2), 165 K (3), 175 K (4), 190 K (5).

exchange-correlation interaction was taken into account by the local density approximation (LDA) in the Perdew-Wang parametric form [13], which reproduces the Ceperley-Alder exact results of the quantum-mechanical calculations for a homogenous electron gas [14]. The non-locality of the pseudopotentials was taken into account by components for the *s*- and *p*-channels for the Br atom with a local *p*-component, for the *s*-, *p*- and *d*-channels for the P and S atoms with local *d*-component, and for the *s*-, *p*- and *d*-channels for the Cu atom with local *s*-component. The nonlinear character of the exchange-correlation interaction of the valence electrons with the electrons in the atomic core and the relativistic effects for the core electrons were included in the pseudopotential. The spin-orbit interaction was not considered in the treatment performed in this work.

The present results have been obtained thanks the use of the ABINIT code [15], that is based on pseudopotentials and planewaves. It relies on an efficient Fast Fourier Transform algorithm [16] for the conversion of wavefunctions between real and reciprocal space, on the adaptation to a fixed potential of the band-by-band conjugate gradient method [17] as well as on a potential-based conjugate-gradient algorithm to determine the self-consistent potential [18]. Technical details on the computation of responses to atomic displacements and homogeneous electric fields can be found in [19], while reference [20] presents the subsequent computation of dynamical matrices, Born effective charges, dielectric permittivity tensors, and interatomic force constants.

Integration over the Brillouin zone (BZ) was performed using the special points method [21]. We used the 2 points in the irreducible part of BZ, which correspond to the shifted 2×2×2 Monkhorst-Pack mesh. The planewave basis set was restricted by the maximum kinetic energy cutoff of 50 Ry. The sufficiency of the chosen basis was checked. The internal structure parameters are optimized by means of Hellmann-Feynman forces with tolerance of 10^{-4} Ry/bohr.

3. Results and discussion

3.1. Raman scattering studies

In the Raman spectrum of Cu_6PS_5Br crystal separate groups of bands are observed. In the low-frequency range (below 100 cm^{-1}) the bands correspond to diffusive-type vibrations of Cu atoms and Cu–Br bond vibrations are observed [4]. In the range near 310 cm^{-1} a broad asymmetric band is observed, which is caused by superimposition of a doubly degenerate E mode and a triply degenerate F_2 mode. At 425 cm^{-1} in the Raman spectra, the band corresponding

to A_1 symmetry vibration is observed, being the most pronounced in the spectra. In the range of $500 - 600$ cm^{-1}, two bands are observed in the spectra, related to TO and LO vibrations of F_2 mode, corresponding to internal stretching vibrations of PS_4^{3-} tetrahedral groups. The low-temperature studies have shown that the most essential changes in Raman spectra are realized in low-frequency range ($\omega < 100$ cm^{-1}) and in the medium ($270 < \omega < 350$ cm^{-1}) range. Figure 1 illustrates the temperature studies of the low-frequency range ($\omega < 100$ cm^{-1}) of Cu_6PS_5Br crystal Raman spectra. It should be noted that the studies of the low-frequency spectral range are most interesting for solid electrolytes, since the low-energy mode observed in phonon spectra is their typical characteristic, generally referred to as the low-energy optical (LEO) phonon [22,23]. The role of the LEO phonon consists in the increase of the vibration amplitude and in supporting the mobile ion hopping, i. e. assisting the realization of an effective ion transport and superionic conductivity. Besides, the LEO phonon reflects the mobile ion motion, which can be observed as a broadening of the corresponding bands at and above the superionic PT.

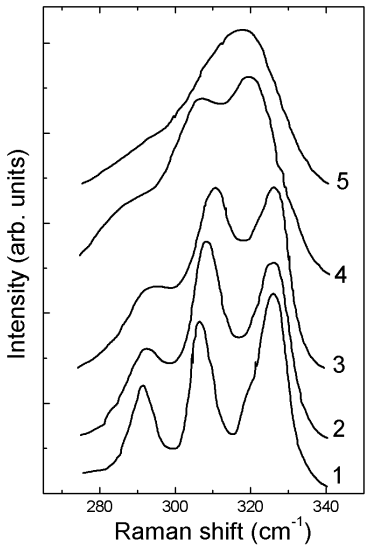

Figure 2. Raman spectra of Cu_6PS_5Br crystal in the range of internal stretching vibrations ($270 < \omega < 350$ cm^{-1}) at the temperatures 77 K (1), 140 K (2), 165 K (3), 175 K (4), 190 K (5).

It is seen in figure 1a that in the low-frequency range, a strong light scattering at $\omega < 20$ cm^{-1} is observed. Hence, the possibility to uncover the true shapes of the spectral bands and to determine their spectral positions and halfwidths is strongly encumbered. Therefore, we applied a procedure that had been successfully used for other solid electrolytes [24–26] where the effect of Bose-Einstein statistic factor, strongly modifying the low-frequency spectral range, was taken into account. The Raman intensity with the account of Bose-Einstein factor is given by

$$I_R(\omega) = I(\omega)\frac{1}{n(\omega,T)+1}\,, \qquad (1)$$

where $I(\omega)$ is the experimentally measured intensity (figure 1 (a)), and the Bose-Einstein factor is as follows:

$$n(\omega,T) = \frac{1}{\exp\left(\frac{\hbar\omega}{k_B T}\right)-1}\,. \qquad (2)$$

Thus the obtained Raman spectra are shown in figure 1b. In the low-frequency part of the spectrum, six bands are observed at 77 K. With temperature, the vibrational bands monotonously shift to lower frequencies and broaden which leads to the reduction of the number of bands observed (see figure 1), and at $T = 155$ K only three bands at $\omega_2 = 36$, $\omega_3 = 53$ and $\omega_5 = 75.5$ cm^{-1} are revealed. In the range of superionic PT at $T_s = 166 - 180$ K we observed the anomalies in the temperature dependences of the band frequencies and a stepwise increase of halfwidths for all the bands. In particular, at the superionic PT halfwidths, Γ_2 and Γ_3 increase almost by 10 cm^{-1}, and Γ_5 – by 20 cm^{-1}. Such a broadening of the Raman bands is explained by dynamical structural disordering of copper cation sublattice at the superionic PT. The results of temperature studies of Cu_6PS_5Br crystal Raman spectra in the range of internal stretching vibrations of PS_4^{3-} tetrahedral groups ($270 < \omega < 350$ cm^{-1}) are shown in figure 2. At $T = 77$ K, four bands are observed in the Raman spectrum, the band at ω_3 being revealed as a shoulder at the low-frequency side of the ω_4 band. With the temperature increase at $T < T_s$, the band at ω_3 is masked by the low-frequency wing of the ω_4 band, and the frequencies ω_1 and ω_2 smoothly increase; the halfwidths of all the bands also increase. In the region of the superionic PT the phonon bands continue to broaden (curve 4 in figure 2, and already at 190 K (curve 5) only one broad band centred at 319 cm^{-1} is observed instead of three high-frequency bands ω_2, ω_3 and ω_4. This band of the vibrational mode of F_2 symmetry remains unchanged at the further increase of temperature to 295 K. Of special

interest is the fact that the triple degeneracy of the vibrational modes in the range near 320 cm^{-1} takes place not at the structural ferroelastic phase transition from monoclinic to cubic syngony $Cc \rightarrow F\bar{4}3m$ which occurs at $T_c = 268$ K, but at an isostructural ($Cc \rightarrow Cc$) superionic PT at the temperature lower almost by 100 K ($T_s = 166 - 180$ K). This effect is explained by strong phonon anharmonicity due to the transition to the superionic state, accompanied by strong broadening of the bands corresponding to stretching vibrations of PS_4 tetrahedra. The band at ω_1 strongly smears at the transition to the superionic state (curve 4 in figure 2), its intensity decreases, and at $T = 190$ K there is observed only as a weak shoulder at the low-frequency side of the band of F_2 symmetry.

3.2. *Ab initio* determination of the crystalline structures

We consider the high-symmetry superionic phase with $F\bar{4}3m$ cubic lattice. Its structure was redetermined by Haznar *et al.* [5] at 295 K and 420 K. A model with an ordered anion sublattice and two sublattices of Cu cations creating disordered network was proposed. Position of Cu atoms is divided between two sites, g and h, with fractional occupancies (see table 1).

Table 1. Comparation of theoretical (present work) and experimental [5] fractional coordinates (in brackets) and corresponding atom occupancies P of Cu_6PS_5Br crystal in high-symmetry configuration. The calculated lattice paramenter is a=9.706 Å. Its difference from the corresponding experimental parameter (a=9.708 Å) is 0.02 %.

Atom	Experiment	P_{exp}	Theory	P_{theor}
Cu(1)	(0.02362, 0.25, 0.25)	62.4	(0.01747, 0.25, 0.25)	100.0
Cu(2)	(0.01914, 0.30918, 0.30918)	37.6		0.0
Br(1)	(0., 0., 0.)	98.9	(0., 0., 0.)	100.0
S(2)	(0.25, 0.25, 0.25)	98.9	(0.25, 0.25, 0.25)	100.0
S(3)	(0.62183, 0.62183, 0.62183)	100.0	(0.62314, 0.62314, 0.62314)	100.0
P(1)	(0.5, 0.5, 0.5)	100.0	(0.5, 0.5, 0.5)	100.0

In the present theoretical investigations we do not consider the structural disordering, making an assumption that all cation atoms are placed in the g-sites, which are fully occupied. Using the $F\bar{4}3m$-symmetry constraint we optimized the lattice parameters and fractional atomic coordinates to the 0 K in order to find the ground-state geometry of the high-symmetry phase. The results of this optimization are collected and compared with the experiment in table 1. An excellent agreement with experiment is achieved in these calculations, although the simulation temperature significantly differs from experimental conditions.

3.3. Vibrational properties

The calculated set of the long-wavelength frequencies of the ordered high-symmetry Cu_6PS_5Br presents two unstable modes, which are mentioned in table 2 by imaginary unity. The presence of these two unstable modes is in excellent agreement with the experimentally observed phase transition sequences:

(i) Optical mode with imaginary frequency 72 cm^{-1} is described by irreducible representation F_2 and is related to the high-temperature phase transition at 270 K, which is ferroelastical in nature. As far as the acoustic vibrations have the same symmetry representation F_2, the mentioned optical unstable mode interacts by its softening with the acoustical ones, leading to the ferroelastical distortion from the cubic lattice to a monoclinic one. Eigenvector of this vibration is mostly characterized by out-of-phase vibrations of the heavy atoms of the lattice: Cu and Br.

(ii) Optical vibration with imaginary frequency 51 cm^{-1} can be associated with experimentally observed superionic phase transition occurring at $166 - 180$ K. Corresponding eigenvector

presents significant displacements only in cation sublattices that lead to the six inequivalent positions with large interatomic distances and to the disappearance of the ionic conductivity.

Table 2. Long wave-length vibrational frequencies (in cm^{-1}) of the Cu_6PS_5Br crystal in the cubic phase

Frequency		
Symmetry	Theory	Experiment
F_2	$72.3i$ (TO); $59i$(LO)	
F_1	$51.7i$ (TO); $20i$(LO)	
F_2	74.2	74
F_1	80.8	78
F_2	109.2	
E	147.6	156
A	206.0	234
F_2	211.0	245
F_1	317.5	
F_2	320.0	316
E	347.0	
F_2	348.9	
A	415.4	427
F_2	511.3(TO); 521(LO)	547(TO); 558(LO)

The displacement pattern of the stable low-energy vibrations with frequency 74 cm^{-1} is built by out-of-phase Cu and Br displacements. In the pattern for 80 cm^{-1}-mode, the atomic displacements of Br and S(2) atoms are zero. In 109 cm^{-1}-mode the displacements of Br atom are negligibly small, whereas the displacement pattern is built by counterphase displacements of Cu, P and S sublattices. E-symmetry 147 cm^{-1}, and A-symmetry 205-cm^{-1} modes are "breathing" with out-of-phase displacements in Cu and S(3) sublattices. In high-energy modes significant displacements are observed for the light P and S atoms forming an anion framework.

The calculated Born effective charges maintain the ionic nature of interatomic bonding in Cu_6PS_5Br: tensor for Cu is anisotropical with the principal values ranging from 0.6 to 0.8; the charge of P atom is 2.72; S(2) has the principal value equal to -0.9 and the charge of S(3) atom is -1.1; Br has the biggest negative charge in the system equal to -2.08. LO–TO splitting is significant only for unstable modes and for the mode with the highest frequency.

4. Conclusions

The temperature studies of Raman scattering spectra in Cu_6PS_5Br crystals have been performed. In the low-frequency range strong light scattering at $\omega < 20$ cm^{-1} is observed. In the range of superionic phase transition at $T_s = 166 - 180$ K the anomalies in the temperature dependences of the band frequencies and a stepwise increase of halfwidths for all the bands are revealed.

Ab initio long-wavelength phonons calculated for high-symmetry cubic structure within density functional perturbation theory show two unstable modes indicating the experimentally observed sequence of ferroelastic and superionic phase transitions. The calculated phonon frequencies and structural parameters have been compared with the available experimental data.

Acknowledgements

K.Z.R. is very appreciated to Alexander von Humboldt Foundation for financial support.

References

1. Kuhs W., Nitsche R., Scheunemann K. Mater. Res. Bull, 1979, **14**, 241.
2. Kuhs W., Nitsche R., Scheunemann K. Acta Cryst. B, 1978, **34**, 64.
3. Studenyak I., Kovacs G., Orliukas A., Kovacs E. Izv. AN: ser. fiz., 1992, **56**, 86.
4. Studenyak I., Stefanovich V., Kranjcec M., Desnica D., Azhnyuk Y., Kovacs G.S., Panko V. Solid State Ionics, 1997, **95**, 221.
5. Haznar A., Pietraszko A., Studenyak I. Solid State Ionics, 1999, **119**, 31–36.
6. Fiechter S., Gmelin E., Thermochimica Acta, 1985, **85**, 155.
7. Skritskiy V., Valyavichius V., Samulionis V., Studenyak I., Kovacs G., Panko V. Fiz. Tverd. Tela, 1989, **31**, 234.
8. Studenyak I., Kranjcec M., Kovacs G., Panko V., Azhnyuk Y., Desnica I., Borets O., Voroshilov Y. Mat. Sci. Eng. B, 1998, **52**, 202.
9. Studenyak I., Kranjcec M., Kovacs G., Panko V., Desnica I., Slivka A., Guranich P. J. Phys. Chem. Solids, 1999, **60**, 1897.
10. Studenyak I., Kranjcec M., Suslikov L., Kovacs G., Guranich P. Optics and Spedroscopy, 2002, **93**, 300.
11. Kohn W., Sham L.J., Phys. Rev. A, 1965, **140**, 1133.
12. Troullier N., Martins J.L. Phys. Rev. B, 1991, **43**, 1993.
13. Perdew J.P., Wang Y. Phys. Rev. B, 1986, **33**, 8800.
14. Ceperley D.M., Alder B.J. Phys. Rev. B, 1980, **45**, 566.
15. Gonze X., Beuken J.-M., Caracas R., Detraux F., Fuchs M., Rignanese G.-M., Sindic L., Verstraete M., Zerah G., Jollet F., Torrent M., Roy A., Mikami M., Ghosez P., Raty J.-Y., Allan D. Computational Materials Science, 2002, **25**, 478–492.
16. Goedecker S. SIAM J. of Scientific Computing, 1997, **18**, 1605.
17. Payne M.C., Teter M.P., Allan D.C., Arias T.A., Joannopoulos J.D. Rev. Mod. Phys., 1992, **64**, 1045.
18. Gonze X., Phys. Rev. B, 1996, **54**, 4383.
19. Gonze X., Phys. Rev. B, 1997, **55**, 10337.
20. Gonze X., Lee C., Phys. Rev. B, 1997, **55**, 10355.
21. Monkhorst H.J., Pack J.D., Phys. Rev. B, 1976, **13**, 5188.
22. Kobayashi M., Tomoyoze T., Aniya M. Physica B, 1996, **219–220**, 460.
23. Wakamura K. Phys. Rev. B, 1999, **59**, 3560.
24. Fontana A., Mariotto G., Rocca F. Phys. Stat. Sol. (b), 1985, **129**, 489.
25. Fontana A., Rocca F., Fontana M. Phys. Rev. Lett., 1987, **58**, 503.
26. Fontana A., Rocca F., Fontana M., Rossi B., Dianoux A. Phys. Rev. B, 1990, **41**, 3778.

Фононні спектри суперіонного сегнетоеластика Cu_6PS_5Br: експериментальні та теоретичні дослідження

І.П.Студеняк[1], К.З.Рущанський[2], Р.Ю.Бучук[1], В.О.Стефанович[2]

[1] Ужгородський національний університет, фізичний факультет,
вул. Підгірна 46, 88000 Ужгород, Україна

[2] Інститут фізики та хімії твердого тіла, Ужгородський національний університет,
вул. Волошина 54, 88000 Ужгород, Україна

Отримано 4 вересня 2006 р.

Експериментально виявлено аномальну температурну поведінку піків раманівського розсіювання світла при суперіонному фазовому переході в Cu_6PS_5Br. Для високосиметричної кубічної фази теоретично розраховано першопринципні частоти довгохвильових фононів з використанням теорії збурень функціонала густини у локальному наближенні. У фононному спектрі спостерігаються дві нестабільні моди, які вказують на експериментально спостережувану послідовність сегнетоеластичного і суперіонного фазових переходів.

Ключові слова: *суперіонні матеріали, динаміка гратки, фазові переходи*

PACS: *63.20.Dj, 64.60.Cn, 78.30.Hv*